
ORIGINAL ARTICLE

Journal Section

Global Output-Feedback Extremum Seeking Control with Source Seeking Experiments

Nerito Oliveira Aminde^{1*} | Tiago Roux Oliveira^{2†} |
Liu Hsu^{3‡}

¹Federal Center for Technological Education "Celso Suckow da Fonseca" (CEFET/RJ), Angra dos Reis, Rio de Janeiro – RJ, 23953-030, Brazil

²State University of Rio de Janeiro (UERJ), Rio de Janeiro – RJ, 20550-900, Brazil

³Federal University of Rio de Janeiro (COPPE/UFRJ), Rio de Janeiro – RJ, 21941-972, Brazil

Correspondence

Nerito Oliveira Aminde
Email: nerito.aminde@cefet-rj.br

Present address

*Department of Electrical Engineering, CEFET/RJ

†Department of Electronics and Telecommunication Engineering, UERJ

‡Program of Electrical Engineering, COPPE/UFRJ

Funding information

CAPES, CNPq, FAPERJ, ISDB-Maputo and CINOP Global

This paper discusses the design of an extremum seeking controller that relies on a monitoring function for a class of SISO uncertain nonlinear systems characterized by arbitrary and uncertain relative degree. Our demonstration illustrates the feasibility of achieving an arbitrarily small proximity to the desired optimal point through output feedback. The core concept involves integrating a monitoring function with a norm state observer for the unitary relative degree case and its expansion to arbitrary relative degrees by means of the employment of a time-scaling technique. Significantly, our proposed scheme attains the extremum of an unknown nonlinear mapping across the entire domain of initial conditions, ensuring global convergence and stability for the real-time optimization algorithm. Furthermore, we provide tuning rules to ensure convergence to the global maximum in the presence of local extrema. To validate the effectiveness of the proposed approach, we present a numerical example and apply it to a source-seeking problem involving a cart-track linear positioning servomechanism. Notably, the cart lacks the ability to sense its velocity or the source's position, but can detect the source of a light signal of unknown concentration field.

KEYWORDS

Extremum Seeking, Source Seeking, Nonlinear Systems, Output Feedback

1 | INTRODUCTION

Extremum seeking control (ESC) is a control system used to determine in real-time the extremum (maximum or minimum) of an unknown nonlinear mapping [1]. ESC has become a key area in control theory due to increasing need to optimize plant operation in order to reduce operating costs and meet product specifications [2, 3]. In [1] and the cited references, numerous applications are discussed, including but not limited to the design of antilock braking systems, autonomous vehicles, mobile robots, internal combustion engines, process control, particle accelerators, and source seeking. Recently, an extension of the scope of applicability of the ESC through delays and PDEs was proposed in [4], with practical engineering scenarios including neuromuscular electrical stimulation [5], non-cooperative games [6], biological reactors [7, 8], oil-drilling systems [9], and flow-traffic control for urban mobility [10].

The prevalent algorithms for unconstrained optimization typically rely on the derivative or gradient of the objective function. Nonetheless, in numerous control problem applications, including those outlined earlier, crucial components such as the plant model, gradient information, and the cost function for optimization are not readily accessible online. Furthermore, "gradient sensors" have a tendency to magnify noise and encounter instability issues, particularly at higher frequencies [11].

Classical ESC methods employ a high-pass filter in the system output along with a small sinusoidal perturbation (dither signal) technique to estimate the gradient of the cost function. This approach is known for its simplicity and rapid adaptation [12, 13, 14]. Nevertheless, only local stability properties could be assured when assuming full-state measurement. In [1, 15, 16], under the identical assumption, semi-global practical convergence was achieved, but with a decrease in the convergence rate within the domain of attraction.

In [17, 18, 19], the extremum seeking could be seen as a nonlinear control challenge featuring a state-dependent high-frequency gain (HFG), which alters direction (referred to as control direction) around the optimal point of interest. In addressing this, a method employing sliding mode control for tracking uncertain plants with an unknown control direction was introduced in [20, 21, 22] using an algorithm of switching based on a monitoring function to the output error. In [23], it was conjectured that the lack of robustness of such monitoring scheme with respect to recurrent changes of HFG sign would preclude the monitoring function to be directly applied to extremum seeking control.

In this paper, a novel monitoring function is proposed in order to show that the output-feedback tracking controller proposed in [20, 21, 22], indeed can also be applied to ESC of a class of uncertain nonlinear systems (of unitary and arbitrary relative degrees), while global convergence properties of the search algorithm are also guaranteed without affecting its rate of convergence. Moreover, the proposed algorithm can be reconfigured to achieve a global extremum point in the presence of local extrema.

On the other hand, the control of systems with uncertain relative degrees is a challenging task. There are few results in the adaptive and sliding mode control literature [24, 25, 26, 27] which consider the model reference and stabilization problems, but not for extremum seeking. Even in those cases the processes are restricted to an uncertainty not exceeding 2, *i.e.*, the uncertain relative degree may be n^* , $n^* + 1$ or $n^* + 2$. As a further contribution of this paper, a generalization is achieved to include more general dynamics with arbitrary and uncertain relative degrees, without using differentiators to compensate them [28, 29, 30, 31]. The theoretical contribution of this paper is to develop a time-scaling procedure in order to reduce the order of the system dynamics, and consequently, to allow the analysis and control design for enlarged uncertainty in the relative degree.

In particular, research in applications that use autonomous vehicles are wide, varied, and constantly growing. Notably, there is a burgeoning interest in researching vehicles that operate without access to precise position information. These vehicles must navigate and perform a desired task without the use of GPS (Global Positioning System) or inertial navigation [32, 33, 34, 35]. A recent solution to this problem was given in the context of source seeking

[33, 34, 36, 37, 38]. This problem has been intensively explored in the robotics literature where results of extremum seeking control [13, 12, 19, 15, 16, 1] are applied to autonomous mobile robots with the objective of localizing the source of an unknown, nonlinear, signal field. For environments where position information is unavailable, the extremum seeking method is applied to autonomous vehicles as a means of navigating to find the source of some signal which the vehicles can measure locally. The signal is at maximum intensity at the source and decreases with distance away from the source. The source signal to be detected may be electromagnetic, acoustic, a temperature intensity or the concentration of a biological/chemical agent [36, 37, 38].

Finally, we conduct experiments to validate the proposed theoretical results. We employ the new ESC scheme based on monitoring functions in a light-source seeking scenario for a one-dimension optimization problem, *i.e.*, both input and output signals are scalar functions. The theoretical results for basic extremum seeking are applied to control a linear servo-positioning system to perform localization and tracking of a light source, without its position/velocity information. Preliminary conference versions were presented in [39, 40].

2 | PRELIMINARIES AND PROBLEM FORMULATION

Throughout the paper, the Euclidean norm of a vector x and the corresponding induced norm of a matrix A are denoted by $\|x\|$ and $\|A\|$, respectively. The term $\pi_i(t)$ stands for any exponential decaying function, such that $|\pi_i(t)| \leq R e^{-\beta t}$, $\forall t$, and some positive scalars R and β . Class \mathcal{K} and \mathcal{K}_∞ functions are defined as in [41]. From a technical standpoint, the theoretical results obtained in this paper are based on Filippov's definition for solution of differential equations with discontinuous right-hand sides [42].

Consider the following nonlinear uncertain system:

$$\dot{x} = f(x, t) + g(x, t)u \quad (1)$$

$$z = h(x, t) \quad (2)$$

in cascade with a static subsystem

$$y = \Phi(z), \quad (3)$$

where $u \in \mathbb{R}$ is the control input, $x \in \mathbb{R}^n$ is the state vector, $z \in \mathbb{R}$ and $y \in \mathbb{R}$ are measured outputs of the first subsystem and of the static subsystem, respectively. In order to assure existence and forward uniqueness of solutions, the nonlinear uncertain functions f , g and h are locally Lipschitz continuous in x , piecewise continuous in t and sufficiently smooth. Without loss of generality, we assume that the initial time is $t = 0$. For each solution of (1) there exists a maximal time interval of definition given by $[0, t_M)$, where t_M may be finite or infinite. The control objective of ESC is not "stabilization" or "tracking", but is "real-time optimization" [16]. However, the ESC problem can be reformulated as a tracking problem in which the control direction is unknown [17]. We wish to find an output-feedback control law u so that, from any initial condition, the system is steered to reach the extremum point y^* and remain on such point thereafter, as close as possible. Without loss of generality, we only address the maximum seeking problem.

The system (1)–(3) can be rewritten in the normal form as follows:

$$\dot{\eta} = \phi_0(\eta, z, t), \quad (4)$$

$$\dot{z} = \phi_1(\eta, z, t) + \phi_2(\eta, z, t)u, \quad (5)$$

$$y = \Phi(z), \quad (6)$$

with state $x := [\eta^T z^T]^T$, $\eta \in \mathbb{R}^{n-1}$ and $z \in \mathbb{R}$, and uncertain nonlinear functions $\phi_0 : \mathbb{R}^{n-1} \times \mathbb{R} \times \mathbb{R}^+ \rightarrow \mathbb{R}^{n-1}$ and $\phi_1, \phi_2 : \mathbb{R}^{n-1} \times \mathbb{R} \times \mathbb{R}^+ \rightarrow \mathbb{R}$.

The state η of the η -subsystem, referred to as an “inverse system”, is not available for feedback.

With respect to the controlled plant, we assume the following assumptions:

(A1) (*On the uncertainties*): All the uncertain plant parameters belong to a compact set Ω .

This assumption is necessary to obtain the uncertainty bounds for control design.

(A2) (*Relative degree one*): The uncertain function $\phi_2(\eta, z, t)$ is bounded away from zero, i.e.,

$$0 < \underline{\phi}_2 \leq |\phi_2|, \quad \forall t \in [0, t_M],$$

where the constant lower bound $\underline{\phi}_2$ is known.

According to (A2), the subsystem (4)–(5) has relative degree one w.r.t. z since $\phi_2 \neq 0$. It restricts us to the case of relative degree one, which is the simplest case amenable by pure Lyapunov design.

By using the notation $\Phi'(z) := \frac{d\Phi(z)}{dz}$ and $\Phi''(z) := \frac{d^2\Phi(z)}{dz^2}$, we consider that (in Ω):

(A3) (*Cost Function*): There exists a unique point $z^* \in \mathbb{R}$ such that $y^* = \Phi(z^*)$ is the extremum (maximum) of $\Phi(z) : \mathbb{R} \rightarrow \mathbb{R}$, satisfying

$$\begin{aligned} \Phi'(z^*) &= 0, \quad \Phi''(z^*) < 0 \\ \Phi(z^*) &> \Phi(z), \quad \forall z \in \mathbb{R}, \quad z \neq z^* \end{aligned}$$

and for any given $\Delta > 0$, there exists a constant $L_\Phi(\Delta) > 0$ such that

$$L_\Phi(\Delta) \leq |\Phi'(z)|, \quad \forall z \notin \mathcal{D}_\Delta := \{z : |z - z^*| < \Delta/2\},$$

where \mathcal{D}_Δ is called Δ -vicinity of z^* and Δ can be made arbitrary small by allowing a smaller L_Φ .

From (5) and (6), the first time derivative of the output y is given by

$$\dot{y} = \Phi' \phi_1 + k_p u, \quad (7)$$

where the plant high frequency gain (HFG), denoted by k_p , is the coefficient of u which appears in the first time derivative of the output y and it is given by

$$k_p = \Phi' \phi_2. \quad (8)$$

As in [17], the $\text{sgn}(k_p)$ is also called *control direction*. The assumption (A3) leads us to consider a nonlinear control system with a state dependent HFG which changes sign around the optimum point of interest in a continuous way.

From (8), (A2) and (A3), k_p satisfies ($\forall z \notin \mathcal{D}_\Delta$)

$$0 < \underline{k}_p \leq |k_p| \quad (9)$$

where the lower bound $\underline{k}_p \leq \underline{\phi}_2 L_\Phi$ is a constant.

(A4) (*Norm observability*): The inverse system (4) admits a known first order norm observer of the form:

$$\dot{\bar{\eta}} = -\lambda_0 \bar{\eta} + \varphi_0(z, t), \quad (10)$$

with z in (5), input $\varphi_0(z, t)$ and output $\bar{\eta}$ such that: (i) $\lambda_0 > 0$ is a constant; (ii) $\varphi_0(z, t)$ is a non-negative function continuous in z , piecewise continuous and upper-bounded in t ; and (iii) for each initial states $\eta(0)$ and $\bar{\eta}(0)$

$$\|\eta\| \leq |\bar{\eta}| + \pi_0, \quad \forall t \in [0, t_M], \quad (11)$$

where $\pi_0 := \Psi_0(|\bar{\eta}(0)| + \|\eta(0)\|) e^{-\lambda_0 t}$ and $\Psi_0 \in \mathcal{K}$.

It is well known that, if the inverse system (4) is input-to-state-stable (ISS) w.r.t. z , then it admits such norm observer and the plant is minimum-phase [43]. More examples of nonlinear systems which satisfies such assumption are given in [17].

In order to obtain a norm bound for the term $\Phi' \phi_1$ in (7), we additionally assume that:

(A5) (*Domination Functions*): There exist known functions $\bar{\Phi}, \alpha_1 \in \mathcal{K}_\infty$, with α_1 locally Lipschitz, a known non-negative function $\varphi_1(z, t)$ continuous in z , piecewise continuous and upper bounded in t such that $|\phi_1(\eta, z, t)| \leq \alpha_1(\|\eta\|) + \varphi_1(z, t)$ and $|\Phi'| \leq \bar{\Phi}(|z|)$.

Note that the Assumption (A5) is not restrictive, since Φ' is assumed to be smooth and ϕ_1 is locally Lipschitz continuous in η and in z . Furthermore, the domination functions α_1 and φ_1 impose stringent growth condition only w.r.t. the time-dependence. Thus, polynomial nonlinearities in η and z can be coped with.

3 | OUTPUT-FEEDBACK EXTREMUM SEEKING CONTROLLER VIA MONITORING FUNCTION

The proposed output-feedback ESC based on monitoring function is represented in Fig. 1. The control law to plants with unknown HFG is defined as in [20, 21]

$$u = \begin{cases} u^+ & = -\rho \operatorname{sgn}(e), \quad t \in T^+, \\ u^- & = \rho \operatorname{sgn}(e), \quad t \in T^-, \end{cases} \quad (12)$$

where the monitoring function is used to decide when u should be switched from u^+ to u^- and vice versa. In (12), ρ is the modulation function to be designed later on and the sets T^+ and T^- satisfy $T^+ \cap T^- = \emptyset$ and $T^+ \cup T^- = [0, t_M]$.

The tracking error e is given by the following

$$e(t) = y(t) - y_m(t), \quad (13)$$

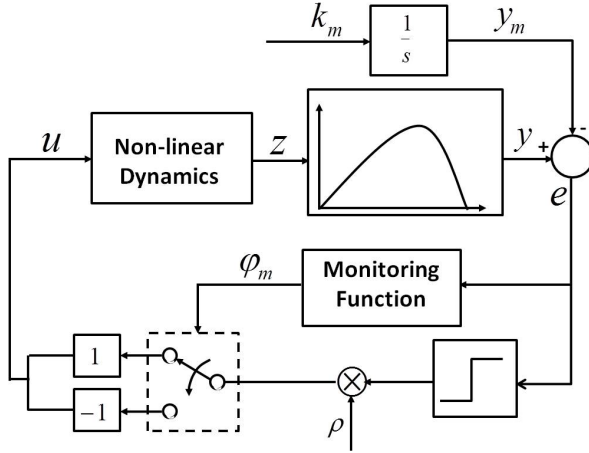


FIGURE 1 Extremum seeking controller using a monitoring function.

where $y_m \in \mathbb{R}$ is a simple ramp time function generated by the reference model

$$\dot{y}_m = k_m, \quad y_m(0) = y_{m0}, \quad (14)$$

where k_m and y_{m0} are design constants. In order to avoid an unbounded reference signal $y_m(t)$ in the controller, one can saturate the model output at a rough known norm upper bound of y^* without affecting the control performance.

The modulation function ρ will be designed so that $y(t)$ tracks $y_m(t)$ as long as possible. In this way, y is forced to achieve the vicinity of the maximum $y^* = \Phi(z^*)$ and remains close to the optimum value y^* . To this end, we have to propose ρ such that the output tracking error e tends to zero in finite time at least outside the Δ -vicinity, that is, in the neighborhood of the maximizer z^* .

Thus, it is straightforward to conclude that $y = \Phi(z)$ tries to track y_m (and consequently y must approach the maximum at y^*) as long as y remains away from a small vicinity of y^* where the HFG is away from zero. In contrast, once y reaches the vicinity of y^* , the HFG will approach zero and thus controllability is lost. Consequently, tracking of y_m will cease. But then the neighborhood of the optimum point is already achieved as desired. Our control strategy will guarantee that y will remain close to y^* thereafter. It is apparent that the convergence rate of z to the Δ -vicinity \mathcal{D}_Δ defined in (A3) is a function of ρ . Although \mathcal{D}_Δ is not positively invariant, after reaching \mathcal{D}_Δ , it will be shown that z will remain close to z^* where the maximum takes place. It does not imply that $z(t)$ remains in $\mathcal{D}_\Delta, \forall t$. However, as shown later on in Theorem 1, one can guarantee that y remains close to the optimum value y^* .

3.1 | Error Dynamics

From (7), (13) and (14), by adding and subtracting λe the time derivative of the error e one has

$$\dot{e} = \Phi' \phi_1 + k_\rho u - k_m + \lambda e - \lambda e, \quad (15)$$

$$\dot{e} = -\lambda e + k_\rho(u + d_e), \quad (16)$$

where $\lambda > 0$ is an appropriate constant and

$$d_e := \frac{1}{k_p} [\Phi' \phi_1 - k_m + \lambda e]. \quad (17)$$

In [22], it is shown that if the control law

$$u = -\text{sgn}(k_p) \rho \text{sgn}(e) \quad (18)$$

was used with modulation function ρ satisfying

$$\rho \geq |d_e| + \delta, \quad (19)$$

modulo exponential decaying terms, then by using the comparison lemma [42], one has $\forall t \in [t_i, t_M)$:

$$|e(t)| \leq \zeta(t), \quad \zeta(t) := |e(t_i)| e^{-\lambda(t-t_i)} + \pi_1, \quad (20)$$

where $\pi_1 := \Psi_1 (|\bar{\eta}(0)| + \|\eta(0)\|) e^{-\lambda_1 t}$, $0 < \lambda_1 < \min\{\lambda_0, \lambda\}$ and $\Psi_1 \in \mathcal{K}$.

On the other hand, if inequality (19) were verified taking into account the exponential decaying terms, the upper bound (20) would be modified to

$$|e(t)| \leq \zeta(t), \quad \zeta(t) := |e(t_i)| e^{-\lambda(t-t_i)}. \quad (21)$$

The major problem is that $\text{sgn}(k_p)$ is unknown in both cases, thus we cannot implement it. In what follows, a switching scheme based on monitoring function is developed to cope with the lack of knowledge of the control direction outside the Δ -vicinity.

3.2 | Monitoring Function Design

The detailed description of monitoring function can be found in [22]. Here, only a brief description of how it works is given. Reminding that inequality (21) holds when the control direction is correct, it seems natural to use ζ in (21) as a benchmark to decide whether a switching of u in (12) from u^+ to u^- (or u^- to u^+) is needed, *i.e.*, the switching occurs only when (21) is violated.

Therefore, consider the following function,

$$\varphi_k(t) = |e(t_k)| e^{-\lambda(t-t_k)} + r, \quad (22)$$

where t_k is the switching time and r is any arbitrary small constant. The monitoring function φ_m can be defined as

$$\varphi_m(t) := \varphi_k(t), \quad \forall t \in [t_k, t_{k+1}) \subset [0, t_M). \quad (23)$$

Note that, from (22) and (23), one has $|e(t)| < |\varphi_k(t)|$ at $t = t_k$. Hence, t_k is defined as the time instant when the

monitoring function $\varphi_m(t)$ meets $|e(t)|$, that is,

$$t_{k+1} := \begin{cases} \min\{t > t_k : |e(t)| = \varphi_k(t)\}, & \text{if it exists,} \\ t_M, & \text{otherwise,} \end{cases} \quad (24)$$

where $k \in \{0, 1, \dots\}$ and $t_0 := 0$ (see Fig. 7).

The following inequality is directly obtained from (23)

$$|e(t)| \leq \varphi_m(t), \quad \forall t \in [0, t_M]. \quad (25)$$

Fig. 2 illustrates the tracking error norm $|e|$ as well as the monitoring function φ_m .

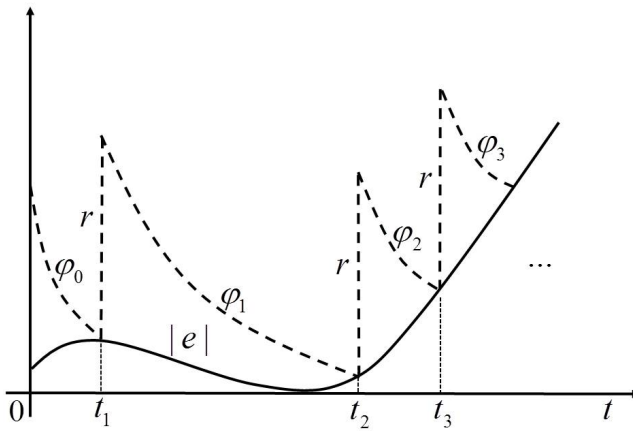


FIGURE 2 The trajectories of $\varphi_m(t)$ and $|e(t)|$.

Main Changes in the Monitoring Function: The main difference with respect to [20, 21, 22] is that the monitoring function previously proposed was based on the upper bound (20) such that φ_k in (22) is replaced by

$$\varphi_k(t) = |e(t_k)|e^{-\lambda(t-t_k)} + a(k)e^{-t/a(k)}, \quad (26)$$

where $a(k)$ is any positive monotonically increasing unbounded sequence. The purpose of the second term in (26) is to dominate the term π_1 which is not available for measurement. In our ESC application it might be a problem since, as will be shown, the ultimate residual set of the proposed algorithm around the maximum y^* is dependent on the values to which the monitoring function converges. Since (26) can assume arbitrarily large values which eventually result in large transients as a result of a change of the control direction and repetitive switching ($k \rightarrow +\infty$). In contrast, this does not occur with the new definition given in (22) whereby the ultimate residual set can be fixed in the order $O(r)$.

3.3 | Modulation Function Design

The following auxiliary available upper bounds provide one possible design for the modulation function so that (19) holds, and they are obtained, taking into account exponentially decaying terms, by using the norm observer given in (A4) and the bounding functions given in (A5).

From (A5) and (11), one has $|\phi_1| \leq \alpha_1 (|\bar{\eta}| + \pi_0) + \varphi_1(z, t)$. Now, note that $\psi(a+b) \leq \psi(2a) + \psi(2b)$, $\forall a, b \geq 0$ and $\forall \psi \in \mathcal{K}_\infty$. Thus, since $\alpha_1 \in \mathcal{K}_\infty$ one can write $\alpha_1 (|\bar{\eta}| + \pi_0) \leq \alpha_1 (2|\bar{\eta}|) + \alpha_1 (2\pi_0)$ and

$$|\phi_1| \leq \alpha_1 (2|\bar{\eta}|) + \alpha_1 (2\pi_0) + \varphi_1(z, t).$$

From (11), $\pi_0 := \Psi_0 (|\bar{\eta}(0)| + \|\eta(0)\|) e^{-\lambda_0 t}$ is uniformly bounded. Thus, since α_1 is assumed locally Lipschitz in (A5), one can obtain a valid linear upper bound for α_1 such that

$$\alpha_1 (2\pi_0) \leq 2k_1 \pi_0 = 2k_1 \Psi_0 (|\bar{\eta}(0)| + \|\eta(0)\|) e^{-\lambda_0 t},$$

where k_1 is a positive constant depending on the Lipschitz constant of α_1 . Then, defining

$$\bar{\phi}_1 := \alpha_1 (2|\bar{\eta}|) + \varphi_1(z, t) \quad (27)$$

and $\bar{\pi}_1 := 2k_1 \Psi_0 (|\bar{\eta}(0)| + \|\eta(0)\|) e^{-\lambda_0 t}$, one can also write

$$|\phi_1| \leq \bar{\phi}_1 + \bar{\pi}_1, \quad (28)$$

where $\bar{\pi}_1$ decays exponentially.

Furthermore, from (28), the first term $\phi_1 \Phi'$ of the y -dynamics in (7) satisfies $|\phi_1 \Phi'| \leq |\Phi'| |\bar{\phi}_1| + |\Phi'| \bar{\pi}_1 \leq |\Phi'| |\bar{\phi}_1| + |\Phi'|^2 + \bar{\pi}_1^2$, where we have used the relationship $|\Phi'| \bar{\pi}_1 \leq |\Phi'|^2 + \bar{\pi}_1^2$. Now, from (A5) the following upper bound holds

$$|\phi_1 \Phi'| \leq \bar{\phi}_1 \bar{\Phi} + \bar{\Phi}^2 + \bar{\pi}_1^2. \quad (29)$$

Remind that, outside the Δ -vicinity, the derivative of the cost function does not vanish $\forall z$. Thus, the lower norm bound \underline{k}_ρ for $k_\rho = \Phi' \phi_2$ given in (9) holds.

Therefore, one can obtain the following norm bound for d_e defined in (17):

$$|d_e(t)| \leq \bar{d}_e + \pi_2 / \underline{k}_\rho, \quad \bar{d}_e := (\bar{\phi}_1 \bar{\Phi} + \bar{\Phi}^2 + k_m + \lambda |e|) / \underline{k}_\rho, \quad (30)$$

with the exponential decaying function $\pi_2 = \bar{\pi}_1^2$.

In the proposed scheme, the following proposition provides one possible modulation function implementation so that (19) holds.

Proposition 1 Consider the system (4)–(6), reference model (14) and control law (12). Outside the Δ -vicinity \mathcal{D}_Δ , if ρ in (12) is designed as

$$\rho := \frac{1}{k_p} \left[\bar{\phi}_1 \bar{\Phi} + \bar{\Phi}^2 + k_m + \lambda |e| \right] + \Pi(k) + \delta, \quad (31)$$

then, while $z \notin \mathcal{D}_\Delta$, one has: **(a)** the monitoring function switching stops, **(b)** no finite-time escape occurs in the system signals ($t_M \rightarrow +\infty$), and **(c)** the error e tends to zero in finite time. The term $\Pi(k) = a(k)e^{-t/a(k)}$ with $a(k)$ being any positive monotonically increasing unbounded sequence and δ is any arbitrary small positive constant.

Proof: Outside the Δ -vicinity, suppose by contradiction that u given by (12) switches without stopping $\forall t \in [0, t_M)$, where t_M may be finite or infinite. Then, $\Pi(k)$ in (31) increases unboundedly as $k \rightarrow +\infty$. Thus, there is a finite value κ such that for $k \geq \kappa$: (i) the term $\Pi(k)$ will upper bound π_2/k_p in (30) and (ii) the control direction is correct. From (i), $\varphi_m(t) > \zeta(t)$, $\forall t \in [t_\kappa, t_{\kappa+1})$, with ζ in (21). From (ii), ζ is a valid upper bound for $|e|$. Hence, no switching will occur after $t = t_\kappa$, i.e., $t_{\kappa+1} = t_M$ (see (24)), which leads to a contradiction. Therefore, φ_m has to stop switching after some finite $k = N$ and $t_N \in [0, t_M)$, whenever $z \notin \mathcal{D}_\Delta$.

Suppose that we end up with an incorrect control direction estimate. Then, the equation for e can be written as $\dot{e} = -\lambda e + |k_p|[\rho \operatorname{sgn}(e) + d_e]$. In this case, if ρ is defined as (31), there exists $t_d < t_M$ such that $e\dot{e} > 0$, $\forall t > t_d$. Hence, e would diverge as $t \rightarrow t_M$ for all initial conditions. Therefore, $\operatorname{sgn}(k_p)$ must be correctly estimated at $k = N$.

Now, consider the quadratic function

$$V_e = \frac{e^2}{2}. \quad (32)$$

Then calculating \dot{V}_e along the solutions of (16),

$$\dot{V}_e = e\dot{e} \quad (33)$$

$$\dot{V}_e = e[-\lambda e + k_p(u + d_e)]. \quad (34)$$

Since the control signal is given by (12) and the $\operatorname{sgn}(k_p)$ was correctly estimated, the function \dot{V}_e can be rewritten as

$$\dot{V}_e = e[k_p(-\operatorname{sgn}(k_p)\rho \operatorname{sgn}(e) + d_e) - \lambda e] \quad (35)$$

$$= e[-|k_p|\rho \operatorname{sgn}(e) + k_p d_e - \lambda e] \quad (36)$$

$$\leq |e||k_p|[-\rho + |d_e| + |k_p^{-1}\lambda e|]. \quad (37)$$

Since the modulation function ρ satisfies (31), the following inequality holds $\dot{V}_e \leq -\delta|k_p||e| < 0$, is valid with a constant $\delta > 0$, and the condition $e\dot{e} < 0$ (or equivalently $\dot{e} = -\lambda_1 \operatorname{sgn}(e)$, for some $\lambda_1 > 0$), is verified such that $e(t) \rightarrow 0$ in finite time, while $z \notin \mathcal{D}_\Delta$. Consequently, it is not difficult to conclude that no finite-time escape can occur, i.e., $t_M = +\infty$. ■

Modulation Function Reset The term $\Pi(k)$ in (31) plays a key role in the domination of the exponential decaying term π_2/k_p in (30). It allows that inequality (19) is satisfied before that π_2/k_p ultimately vanishes. However, since $\Pi(k) \rightarrow +\infty$ as $k \rightarrow +\infty$, the modulation function needs a reset mechanism to reinitialize k , from time to time, in order to avoid that the controller amplitudes increase to very high values. In particular, if a first order nonlinear system is considered (i.e., the η -dynamics in (4)–(6) is dropped), the term $\Pi(k)$ can be removed.

3.4 | Global Convergence Result

In the next theorem, we show that the proposed output-feedback controller based on monitoring function drives z to the Δ -vicinity of the unknown maximizer z^* defined in **(A3)**. It does not imply that $z(t)$ remains in \mathcal{D}_Δ , $\forall t$. However, the oscillations around y^* can be made of order $O(r)$.

Theorem 1 Consider the system (4)–(5), with output or cost function in (6), control law (12), modulation function (31), monitoring function (22)–(23) and reference trajectory (14). Assume that **(A1)**–**(A5)** hold, then: (i) the Δ -vicinity \mathcal{D}_Δ in **(A3)** is globally attractive being reached in finite time and (ii) for L_Φ sufficiently small, the oscillations around the maximum value y^* of y can be made of order $O(r)$, with r defined in (22). Since the signal y_m can be saturated in (14), all signals in a closed-loop system remain uniformly bounded.

Proof: Outside the Δ -vicinity, the derivative of the cost function $\Phi(z)$ does not vanish ($d\Phi(z)/dz \neq 0, \forall z \notin \mathcal{D}_\Delta$). Thus, a lower norm bound \underline{k}_p for k_p can be obtained from the lower bound L_Φ given in **(A3)** which is valid globally. Furthermore, Proposition 1 holds while z stays outside the Δ -vicinity, i.e., no finite-time escape occurs for the system signals.

Now we proceed to the proof of the properties (i) and (ii) of Theorem 1.

(i) Attractiveness of \mathcal{D}_Δ

This proof is made by contradiction. Assume that $z(t)$ stay outside the Δ -vicinity for all t , i.e., $z \notin \mathcal{D}_\Delta, \forall t \in [0, t_M]$. Then, from Proposition 1, there exists a finite time t_s such that $\dot{e} = -\lambda_1 \text{sgn}(e)$, for some $\lambda_1 > 0, \forall t \geq t_s$. The error $e = y - y_m$ tends to zero, but since y_m strictly increases with time and $y = \Phi(z)$ has a maximum value y^* , for t large enough, $y_m > y^* \geq y$ and $\text{sgn}(e) = -1$, assuring that y increases with constant rate ($\dot{y} = k_m + \lambda_1$), from (13)–(14), that is, y must approach y^* . So, z is driven inside \mathcal{D}_Δ , which is a contradiction. Thus, \mathcal{D}_Δ is attained in some finite time. Consequently, $z(t)$ remains or oscillates around \mathcal{D}_Δ , and similarly y with respect to some small vicinity of y^* , $\forall t$ large enough.

These oscillations come from the loss of control strength as $k_p \rightarrow 0$ whenever the relation $\underline{k}_p \leq |k_p|$ is violated, or are due to the recurrent changes in the HFG sign at the extremum point (z^*, y^*) where $k_p = 0$ ($d\Phi(z)/dz = 0$). In what follows, we show that these oscillations can be made ultimately of order $O(r)$, with r from (22).

(ii) Oscillations of order $O(r)$ around y^*

According to the Assumption **(A3)**, Δ can be made arbitrary small so that $|y - y^*| = O(r)$ when $z \in \mathcal{D}_\Delta$. Thus, if $z(t)$ remains in $\mathcal{D}_\Delta, \forall t$, the corresponding neighborhood of y^* can be made of order $O(r)$ with an appropriate L_Φ . Otherwise, the key idea is to show that, if z oscillates around \mathcal{D}_Δ , this also holds since the time spent outside after leaving the set \mathcal{D}_Δ is also of order $O(r)$.

Indeed, first reminding that after some finite time $t_{y^*} > 0$, one has that $\text{sgn}(e) = -1$, since y_m strictly increases with time and $y = \Phi(z)$ has a maximum value y^* . Remind that the output error is given by

$$e(t) = y(t) - y_m(t), \quad \forall t > t_{y^*}. \quad (38)$$

Now, assume that z reaches the frontier of \mathcal{D}_Δ (from inside) at some time $T_1 > t_{y^*}$ with wrong control direction at $t = T_1$. Note that \mathcal{D}_Δ is invariant when the control direction is correct and t is large enough.

Moreover, from (38), one can write

$$\bar{e}(t) = \bar{y}(t) - \delta_m(t - T_1), \quad (39)$$

where $\bar{e}(t) := e(t) - e(T_1)$, $\bar{y}(t) := y(t) - y(T_1)$, $\delta_m = 0$ when y_m is saturated and $\delta_m = k_m$, otherwise.

In addition, from (39) one can also write

$$|\bar{y}(t)| \leq |\bar{e}(t)| + \delta_m(t - T_1). \quad (40)$$

Let $T_2 \geq T_1 > t_{y^*}$ and $T_3 \geq T_1 > t_{y^*}$, where T_2 is the first time when $\varphi_m(t) = e(t)$ (independently if $z(t)$ is inside or outside \mathcal{D}_Δ) and T_3 is the first time when $z(t)$ reaches the frontier of \mathcal{D}_Δ again (from outside). Notice that, $z(t) \notin \mathcal{D}_\Delta$ for $t \in [T_1, T_3]$.

Now, consider two cases: **(a)** z reaches the frontier of \mathcal{D}_Δ with correct control direction ($T_3 > T_2$) and **(b)** z reaches the frontier of \mathcal{D}_Δ with wrong control direction ($T_3 \leq T_2$).

For **case (a)**, suppose $t \in [T_1, T_3]$ and first consider $t \in [T_1, T_2]$. During this time, the control law has wrong control direction. Thus, allowing t_{y^*} to be large enough so that the exponential term π_2/k_p has been dominated by the term $\Pi(k)$ in the modulation function ρ in (31). Consequently, by the construction of the monitoring function, one has $e(T_1) < e(t) < e(T_2)$ and $e(T_2) - e(T_1) < 2r$. Otherwise, a change of control direction would occur according to Proposition 1. Therefore, $\bar{e}(t) = e(t) - e(T_1)$ is of order $O(r)$, $\forall t \in [T_1, T_2]$. Moreover, since $\text{sgn}(k_p)$ was wrongly estimated, one can write $|u(t)| = \rho(t)$, $\forall t \in [T_1, T_2]$, with the control u defined in (12).

From (16), (17), (30) and reminding that t_{y^*} is considered large enough so that the exponential term π_0 has decreased to an arbitrary small value, one can verify that $|\dot{e}| \geq k_p|u + d_e|$ and $|u + d_e| \geq \rho - |d_e| \geq \delta$ with an appropriate positive constant δ in (31).

Hence, $|\dot{e}(t)| > \delta_1$, $\forall t \in [T_1, T_2]$, and $(t - T_1) \leq |\bar{e}|/\delta_1$, where $\delta_1 = k_p \delta$ is an arbitrary positive constant.

Then, reminding that \bar{e} is of order $O(r)$, $\forall t \in [T_1, T_2]$, one can also assure that $(t - T_1)$ and $\bar{y}(t)$ in (40) are of order $O(r)$, $\forall t \in [T_1, T_2]$.

Moreover, by continuity, $\bar{y}(t)$ is also of order $O(r)$, $\forall t \in [T_1, T_2]$. Now, consider $t \in [T_2, T_3]$. During this interval, the control direction is correct σ is in sliding motion, and thus $e \rightarrow 0$. From (38) and (14), one has that $\dot{y} = k_m + \lambda_1 > 0$ and $y(t)$ is strictly increasing, $\forall t \in [T_2, T_3]$. Consequently, one can conclude that $\bar{y}(t) = y(t) - y(T_1)$ is also of order $O(r)$, $\forall t \in [T_2, T_3]$, since $y(t)$ approaches y^* during the latter interval. Since this is also valid for the interval $[T_1, T_2]$, we have proved that the oscillation outside \mathcal{D}_Δ is of order $O(r)$ in case (a), $\forall t \in [T_1, T_3]$.

For **case (b)**, suppose $t \in [T_1, T_3]$. During this time interval, the control law has wrong control direction. Thus, one can also conclude that $\bar{y}(t)$ are of order $O(r)$, $\forall t \in [T_1, T_3]$, following directly the steps of the first part of the proof of case (a). By the continuity of the uncertain output function $y = \Phi(z)$, the boundedness of y stated above implies that z is uniformly norm bounded (\mathcal{UB}), and also from **(A4)** one can easily conclude that all closed-loop system signals are uniformly bounded. ■

3.5 | Multiple Extrema Envisage

ESC applied to achieve global maximum in the presence of local extrema is a challenging area. Sometimes, the exhaustive search of the solution set may be the only choice, as discussed in [16]. The authors have presented a scalar extremum seeking feedback controller that achieves semi-global practical global extremum seeking despite local extrema.

Inspired by the ideas introduced there, it was observed that by tuning a new design parameter in the monitoring function properly, it is possible to pass through a local extremum and converge to the global one as well as is done in [16], when the amplitude of the excitation (dither) signal is adaptively adjusted.

In this case, the monitoring function (22)–(23) should be replaced by

$$\varphi_k(t) = |e(t_k)|e^{-\lambda(t-t_k)} + r + c(k), \quad (41)$$

where $c(k)$ is any positive monotonically decreasing sequence, such that $c(k) \rightarrow 0$ as $k \rightarrow +\infty$, and $c(0) > \mathcal{O}(r)$.

3.6 | Illustrative example

Example 1 Consider in this example a plant with an unknown output performance characteristic and relative degree one dynamics described by

$$\dot{x} = \begin{bmatrix} -1 & 1 \\ 1 & 1 \end{bmatrix} x + \begin{bmatrix} 0 \\ 1 \end{bmatrix} u \quad (42)$$

$$y = \Phi(z) = e^{-\frac{(z-3)^2}{0.5}} + 1.5e^{-\frac{(z-5)^2}{1.5}}, \quad (43)$$

where $x = [\eta^T z]^T$.

The structure of this problem closely resembles various real-world goals, such as fine-tuning a one-dimensional engine calibration. In this scenario, the objective is to determine the optimal valve timing that maximizes efficiency [1]. Note that the performance map shown in Fig. 3 has multiple maxima, and, in contrast to [1], global convergence (for all domain of initial conditions) can be guaranteed.

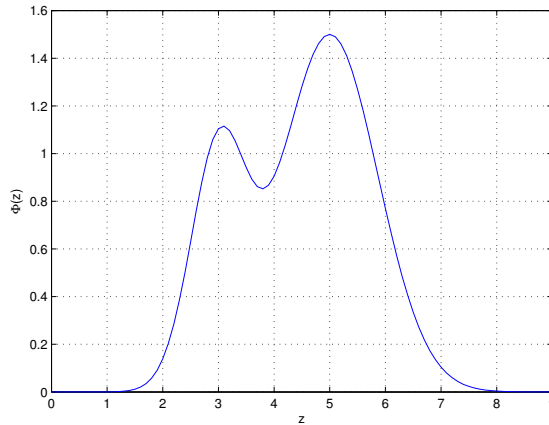


FIGURE 3 Performance map $\Phi(z)$.

The modulation function was designed to satisfy (31) with $\Pi(k) = (k+1)e^{-t/(k+1)}$. The norm observer applied to determine $\bar{\eta}$ used in $\bar{\varphi}_1(\bar{\eta}, z, t)$ has $\lambda_0 = 0.8$ and $\varphi_0(z, t) = 2z$. The monitoring function (41) used to face the problem of local extrema has $c(k) = 2/(k+1)$. The remaining parameters were: the lower bound $L_\Phi = \frac{2}{3}$, $\lambda = 2$, $k_m = 1$, $\delta = 0.1$ and $r = 0.1$.

Fig. 4 illustrates the convergence of the scheme for different initial conditions of x , corresponding to $z(0) = 2, 4$ and 7 . Note that, differently from [1] (see Fig. 6), where the convergence rate and global maximum are directly dependent on the initial conditions, here the example illustrates that it is possible to reach the global maximum in the presence of a local maximum without affecting the rate of convergence and independently of the initial conditions. As shown in Fig. 5, y tracks y_m until z reaches the vicinity of the global maximizer $z^* = 5$. In Fig. 3, the small oscillation just after $t = 1$ s shows the capacity of the monitoring function to pass through a local maximum at $y = 1.1$ and converge to the global one at $y = 1.5$. Fig. 7 illustrates the monitoring function behavior. It can be seen that after reaching the global maximum, the error starts increasing because the reference trajectory is a ramp.

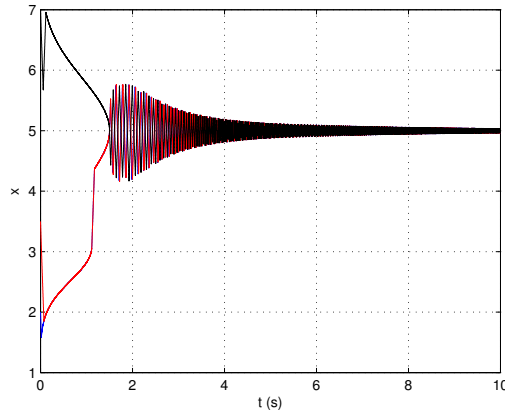


FIGURE 4 Parameter z converges to $z^* = 5$ that maximizes y using different initial conditions $z(0)$.

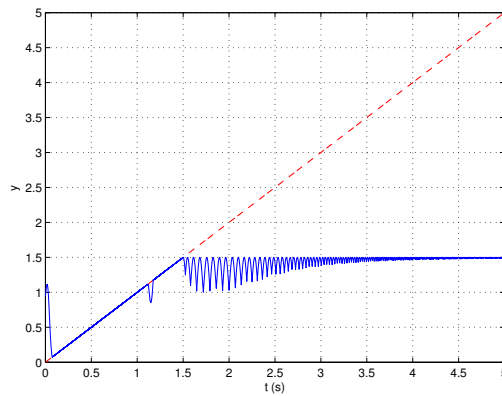


FIGURE 5 Time history of the output plant y (solid line) and the output model y_m (dashed line). The output plant tends to the maximum value $y^* = 1.5$.

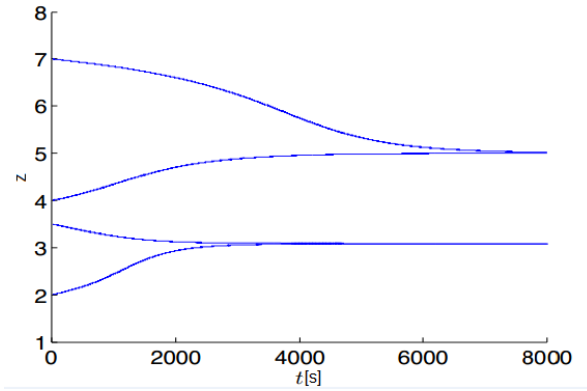


FIGURE 6 Figure extracted from [1]. Convergence of z to local maxima for different values of $z(0)$.

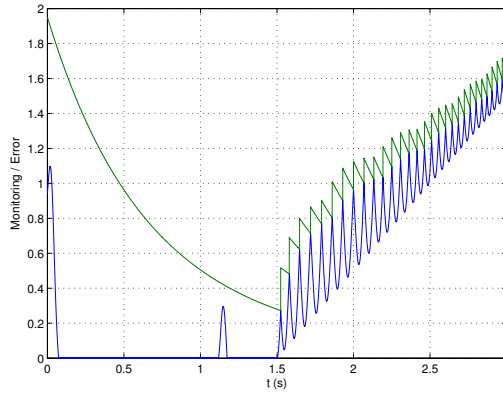


FIGURE 7 Monitoring function φ_m and error norm $|e|$.

4 | UNCERTAIN AND ARBITRARY RELATIVE DEGREES

Relative degree mitigation and the extremum searching are achieved by means of a time-scaling technique. For the sake of simplicity, we restrict ourselves to linear and stable plant dynamics [44], but assuming that the relative degree can be uncertain and arbitrary. By using a singular perturbation method, it is shown that in the new time-scale, an attractive manifold is revealed, which essentially reduces the considered system to a single integrator perturbed by a fast sensor dynamics, which in turn ultimately converges to a small residual set. We then exploit this particular structure to redesign, with reduced control authority, our original control law in Section 3 to show its robustness with respect to the arbitrary relative degree dynamics at the expense of time dilation, which slows down the system response.

In this sense, we intend to show that the ESC proposed in Section 3 can also be extended to systems with

uncertain and arbitrary relative degree (n^*) in the form:

$$\dot{v} = u, \quad (44)$$

$$\dot{x} = Ax + Bv, \quad (45)$$

$$z = Cx, \quad (46)$$

in cascade with a static subsystem

$$y = \Phi(z), \quad (47)$$

where $u \in \mathbb{R}$ is the control input, $x \in \mathbb{R}^n$ is the state vector, $z \in \mathbb{R}$ is an unmeasured output of the linear subsystem (44)–(46) and $y \in \mathbb{R}$ is a measured output of the static subsystem (47), respectively.

Chattering Alleviation: *The integrator in (44) is used to obtain a virtual control signal $v \in \mathbb{R}$, which increases the relative degree of the system [28], i.e., $n \geq n^* - 1$ instead of $n \geq n^*$. The increase of the relative degree yields high-frequency switching in the control u , while the virtual control v driving directly the plant is continuous. Thus, chattering attenuation is expected to be improved [45].*

The matrices $A \in \mathbb{R}^{n \times n}$, $B \in \mathbb{R}^n$, $C \in \mathbb{R}^{1 \times n}$ and the order n of the subsystem (45) may also be uncertain. The uncertain nonlinear function $\Phi : \mathbb{R} \rightarrow \mathbb{R}$ to be maximized must still satisfy the Assumption (A1). The matrix A in (45) must be Hurwitz, to guaranty the uncertainty bounds for control design.

4.1 | Singular Perturbation Analysis

We start summarizing some results obtained in Section 2 for systems with relative degree one. Consider the simplest case of the integrator below with a nonlinear output mapping:

$$\dot{z} = u, \quad (48)$$

$$y = \Phi(z), \quad (49)$$

where $u \in \mathbb{R}$ is the control input, $z \in \mathbb{R}$ is the state vector and $y \in \mathbb{R}$ is the measured output of the static subsystem. In order to present such generalization, consider the system (48)–(49), with the change of variables $z = v$, such that

$$\dot{v} = u, \quad (50)$$

$$y = \Phi(v), \quad (51)$$

can be directly controlled by the method of monitoring function described in Section 3.2.

By using the singular perturbation approach [46], it can be shown that the monitoring function method for ESC (see Section 2) is robust to fast unmodeled dynamics such that the perturbed system (50)–(51) is rewritten in the

following *block sensor form* [46, p. 50]

$$\dot{v} = u, \quad (52)$$

$$\mu \dot{x} = Ax + Bv, \quad (53)$$

$$y = \Phi(Cx), \quad (54)$$

and ultimately satisfies the inequality

$$|y - y^*| \leq O(\sqrt{\mu}), \quad (55)$$

where $\mu > 0$ is a sufficiently small constant. The complete demonstration of (55) follows the same steps presented in [47, 48].

In the singular case $\mu = 0$, the differential equation (53) is replaced by the algebraic equation $x = -A^{-1}Bv$ and, from (52) and (54), the first time derivative of the output signal y is given by

$$\dot{y} = k_p(z)u, \quad (56)$$

where the HFG is now rewritten as

$$k_p(z) = -\Phi'(z)CA^{-1}B. \quad (57)$$

From (57) and (A3), $k_p(z)$ satisfies

$$|k_p(z)| \geq \underline{k}_p > 0, \quad \forall z \notin \mathcal{D}_\Delta, \quad (58)$$

where $\underline{k}_p \leq L_\Phi |CA^{-1}B|$ is a known constant lower bound for the HFG, considering all the admissible uncertainties in $\Phi(\cdot)$, A , B , and C .

4.2 | Time-Scaling for Control Redesign

Thus, by applying an appropriate linear time-scaling [49]

$$\frac{dt}{d\tau} = \mu, \quad (59)$$

the system (52)–(54) can be rewritten as

$$v' = \mu u \quad (60)$$

$$x' = Ax + Bv, \quad (61)$$

$$z = Cx, \quad (62)$$

$$y = \Phi(z), \quad (63)$$

where $v' := \frac{dv}{d\tau}$ and $x' := \frac{dx}{d\tau}$. It means that $\exists \mu^* > 0$ such that the input signal u can be scaled (60) to control the

original system (45)–(47) in a different dilated time-scale governed by $t = \mu\tau, \forall \mu \in (0, \mu^*]$.

The significance lies in the fact that the monitoring function-based ESC, initially designed for systems with a relative degree of one, demonstrates robust to rapid unmodeled stable dynamics ($\mu \rightarrow +0$). Consequently, it proves suitable for controlling dynamics of arbitrary relative degree when appropriately scaled. However, it's anticipated that as $\mu \rightarrow +0$, the trade-off is a slower response of the closed-loop system.

4.3 | Scaled Controller Parameters

The time-scaling (59), allows us to consider the original plant (45)–(47) in a different time-scale being controlled by the controller (12) properly scaled by μu , see (60).

In order to incorporate it, the modulation function must be redesigned to satisfy

$$\rho \geq \mu[|d_e| + \delta], \quad (64)$$

instead of (19).

Remind that the derivative of the objective function does not vanish $\forall z$ outside the Δ -vicinity. Thus, the lower norm bound \underline{k}_p for k_p given in (58) holds.

Therefore, one can obtain the following norm bound as d_e defined in (17):

$$|d_e(t)| \leq \bar{d}_e, \quad \bar{d}_e := (k_m + \lambda|e|)/\underline{k}_p. \quad (65)$$

In the proposed scheme, the following proposition provides one possible modulation function implementation so that (64) holds.

Proposition 2 Consider the system (44)–(47), the reference model (14) and control law (12). Outside the Δ -vicinity \mathcal{D}_Δ , if ρ in (12) is designed as

$$\rho := \frac{\mu}{\underline{k}_p} [k_m + \lambda|e|] + \mu\delta, \quad (66)$$

for μ sufficiently small, then, while $z \notin \mathcal{D}_\Delta$, one has: **(a)** the switching of the monitoring function (22)–(23) stops, **(b)** no finite-time escape of the system signals occurs, which implies that $t_M \rightarrow +\infty$, and **(c)** the error $e(t)$ tends to zero in finite time. The term $\delta > 0$ is any arbitrary constant.

Proof: By considering the singular perturbation argument and the time-scaling (59), which show that the systems (52)–(54) and (60)–(63) are equivalent for μ sufficiently small, then, the demonstration for the original plant (44)–(47) follows the same steps presented in the proof of Proposition 1 for the relative degree one case. ■

Tuning Rules: Since the control design is developed in the light of the slow time-scale μt , it is natural that the parameters k_m of the reference model (14) and λ of the monitoring function (22)–(23) are appropriately scaled, i.e., replaced by μk_m and $\mu\lambda$, respectively. In our ESC application, the ultimate residual set of the proposed algorithm around the maximum y^* is dependent on the values to which the monitoring function converges. According to the definition given in (22), the ultimate residual set r must be of order $O(\sqrt{\mu})$ to satisfy (55).

4.4 | Global Convergence Result

The following theorem states that the proposed output-feedback controller based on monitoring function drives z to the Δ -vicinity defined in (A1) of the unknown maximizer z^* . It does not imply that $z(t)$ remains in $\mathcal{D}_\Delta, \forall t$. However, the amplitude of signal oscillations around y^* can be kept of order $O(\sqrt{\mu})$.

Theorem 2 Consider the system (45)–(46), with output or objective function in (47), control law (44) and (12), modulation function (66), monitoring function (22)–(23) and reference model (14). Assume that (A1)–(A3) hold, then: (i) the Δ -vicinity \mathcal{D}_Δ in (A1) is globally attractive being reached in finite time and (ii) for $L_\Phi(\mu)$ in (A1) sufficiently small, the oscillations of $y(t)$ around the maximum value y^* can be made of order $O(\sqrt{\mu})$, with r defined in (22) being also a constant of order $O(\sqrt{\mu})$. Since the signal y_m can be saturated in (14), all signals in closed-loop system remain uniformly bounded.

Proof: As in the proof of Proposition 2, the demonstration is based on singular perturbation/time-scaling arguments and follows the steps presented in the proof of Theorem 1, for μ sufficiently small. ■

5 | LIGHT SOURCE SEEKING EXPERIMENTS

The basic components utilized in the experiments involving linear motion comprise the cart and track are depicted in Figs. 8, 9 and 10, provided by Quanser Consulting (Linear Position Servo module IP01). The setup includes a cart that smoothly glides along a stainless steel shaft on the ground. Within the cart, a DC motor and a potentiometer are integrated. These components are interconnected through a rack and pinion mechanism: the DC motor contributes the driving force to the system, while the potentiometer facilitates the measurement of the cart's position. The motor shaft is connected to a gear with a diameter of 0.5", and the potentiometer shaft is connected to a gear with a diameter of 1.17". Both gears engage with a toothed rack. As the motor rotates, the torque generated at the output shaft is transformed into a linear force, initiating the movement of the cart. Concurrently, as the cart advances, the potentiometer shaft undergoes rotation, and the voltage, denoted as (e_p), measured from the potentiometer can be calibrated to determine the position (p), i.e., $e_p = 10.7p$, along the track.

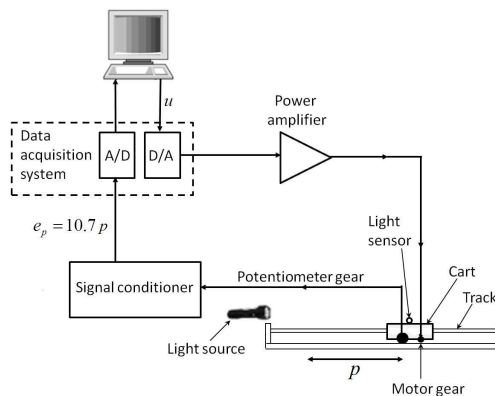


FIGURE 8 Block diagram of the source seeking experiment.

The control algorithm was implemented in a digital computer using the Euler integration method with $1ms$ step size. The car position (ρ) is measured by a potentiometer connected to a 12 bit A/D converter through a signal conditioner, which reduces aliasing and keeps measurement noise amplitude $< 0.4mm$ peak-to-peak. The control signal (u) is a voltage generated by a 12 bit D/A converter connected to a linear power operational amplifier, which drives the DC motor. The saturation limits the control signal peak amplitude to $10V$.

The objective of our feedback system for source-seeking is to regulate the cart's position without relying on data from the potentiometer. Instead, it utilizes the light intensity received by a photosensor, which is also mounted on the top of the cart, as illustrated in Fig. 10. The output from the photosensor undergoes filtration through a low-pass RC filter to eliminate high-frequency noise. It's important to note that the position signal derived from the potentiometer will solely serve the purpose of monitoring system variables in our experiments, without contributing to the design of the control. Simply put, the control designer lacks information about both the cart's position and the source position.

Uncertain Relative Degree: *The breakdown of a controlled system into distinct components: actuator, plant, and sensor is unique. Take, for instance, the flexibility to integrate any actuator or sensor directly into the plant. This integration can significantly alter the relative degree [50], underscoring the importance of the chosen control strategy. A notable drawback of conventional sliding mode-based control methods is their reliance on a precisely defined, constant, and known relative degree for the sliding variable. Even minor disturbances or inaccuracies in the model can cause a reduction in the relative degree or its complete elimination [50, 51].*

In what follows, we evaluate the effectiveness of the proposed controller based on monitoring function and time-scaling under perturbations of external lighting conditions (the light of the laboratory was not turned off during the essays). The performance has also been shown to be robust with respect to the presence of the actuator and sensor dynamics [36], which can be included in the design stage as a part of the linear subsystem (45).

The DC motor of our experimental scenario is essentially modelled as a linear plant with the following nominal first order transfer function:

$$G_p(s) = \frac{z}{v} = \frac{3.9}{(s + 17.2)}, \quad (67)$$

where z is the angular velocity in rpm , the armature voltage v is the control input and the model parameters are considered uncertain in the control design.

The state-space equation of the overall system considering the integrator (44) for chattering alleviation, the relative degree one dynamics (67) of the DC motor and the unknown nonlinear field $\Phi(\cdot)$ created by the light source can be written as

$$\dot{v} = u \quad (68)$$

$$\dot{z} = -17.2z + 3.9v \quad (69)$$

$$y = \Phi(z), \quad (70)$$

where only the output y measured by the photosensor is assumed available for feedback in our experiments. The maximum of $\Phi(z)$ occurs near of the light source, *i.e.*, where the gradient of the field is practically null. The main idea for the control law is to guide the cart up the gradient of the signal to find the source.

Two experiments were conducted in this study. The primary experiment aimed to confirm the effectiveness of the proposed controller in localizing a stationary light source (see Fig. 9). The secondary experiment focused on assessing the tracking capabilities of the proposed ESC when the light source was in motion (Fig. 10).

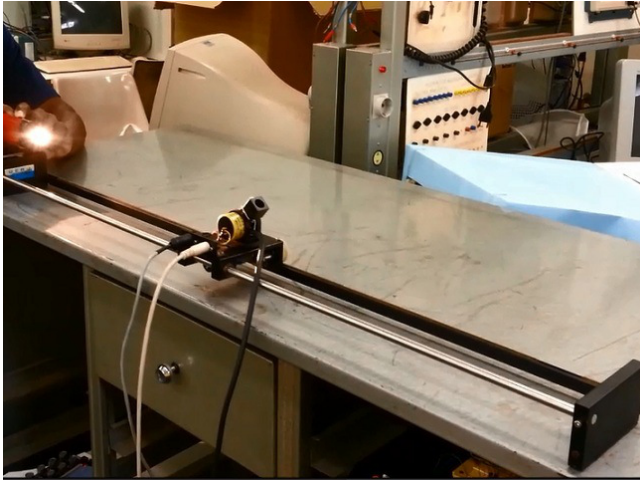


FIGURE 9 Experiment *I*: fixed light source.

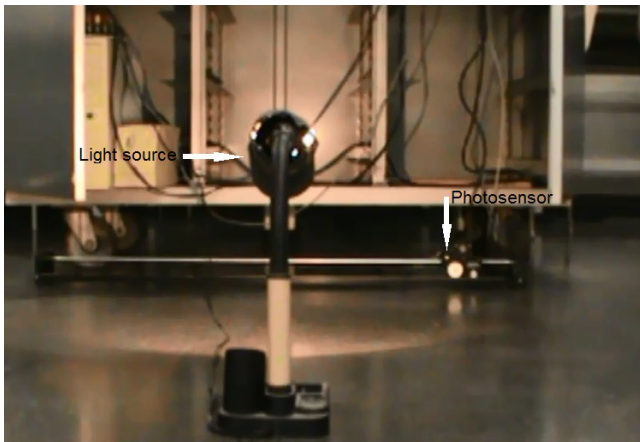


FIGURE 10 Experiment *II*: moving light source.

In both experiments, the reference signal was chosen as in (14) with $k_m = 2\mu$ and y_m was saturated at 5 since this was the maximum light intensity given by the circuit of the photosensor, see Fig. 11. Consequently, e is uniformly bounded.

The monitoring function (22) used to solve our source seeking problem has $\lambda = \mu$ and $r = 0.2\sqrt{\mu}$. The modulation function in the control law (12) was designed to satisfy (66). In this case, the controller parameters could be: $\underline{k}_p = 0.2L_\Phi$, $L_\Phi = 20r$, $\delta = 0.1$ and $\mu = 0.5$.

The discrete-time implementation of the controllers and unmodeled dynamics induce the chattering phenomenon [45] seen in the control signal (Fig. 12). However, it is not a problem since the control signal v applied to the plant is

smooth (curve not shown) due to the integral action in (68) used to reduce control chattering, see Remark 2.

In what follows, we discuss in detail only the results of Experiment II. In this experiment, the light source is positioned in front of the track at a distance of approximately 1 m (Fig. 10). The ESC moves the cart along of the track to search the point of maximum light power.

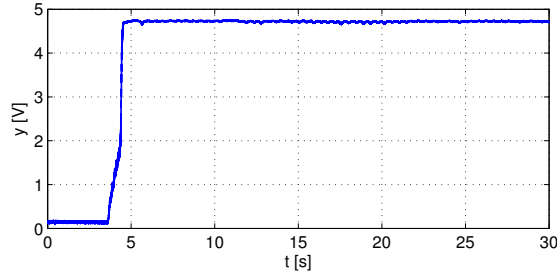


FIGURE 11 Moving source: light intensity received by the photosensor.

Fig. 11 presents the corresponding output voltage of the light intensity y received by the photosensor. Notice that in the initial response up to $t = 4\text{ s}$, the light source was turned off. The residual set captured within this time interval is due to the ambient light. After that, the light source is turned on and the measurement keeps almost constant even when the source is moved and the cart tries to maximize the light intensity Φ which is being measured, see Fig. 13.

Fig. 12 illustrates the temporal evolution of the control signal. Prior to the activation of the light source, there is noticeable high-frequency switching of the control direction due to a violation of an inequality condition (21). This phenomenon arises because the output error $e(t)$ tends to increase while the reference signal $y_m(t)$ saturates at 5 volts, leading to a larger error signal during the initial phase, as indicated in Fig. 6. Additionally, Fig. 6 reveals a transition to lower frequency switching of the control direction between $t = 0$ and 10 seconds, coinciding precisely with the detection of the maximum power point of the light source. Subsequently, the cart settles into oscillations around this point. Furthermore, Fig. 6 provides insight into the behavior of the monitoring function $\varphi_m(t)$ and the output error norm during the movement of the light source, as described earlier.

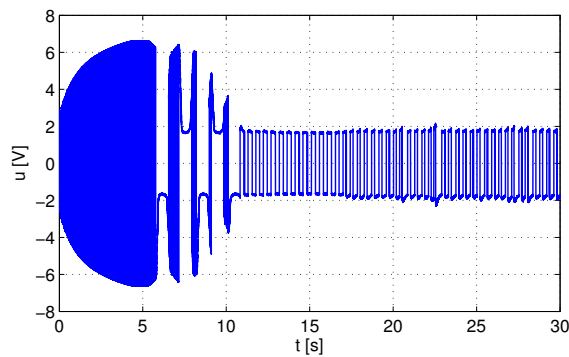


FIGURE 12 Control signal $u(t)$.

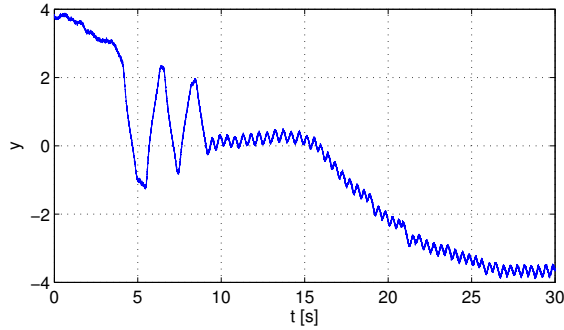


FIGURE 13 Cart position $\rho(t)$ along of the track.

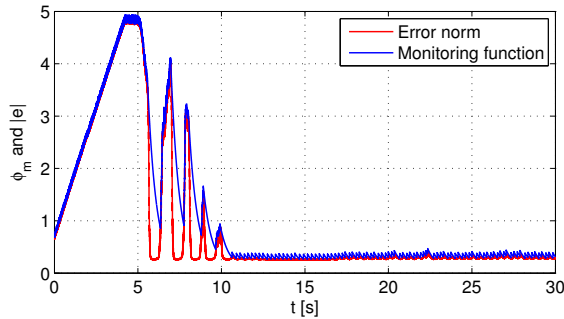


FIGURE 14 Time history of $\varphi_m(t)$ and $|e(t)|$ when the light sensor is moving during the experiment.

Fig. 13 illustrates the cart position during the experiments. For $t \in [0, 4]$, the cart is practically stopped. Immediately after the photosensor has detected the presence of the light source, the cart is moved into its direction and oscillates with decreasing amplitudes around the light source until to reach the ultimate residual set of order $O(r)$. Since the ESC algorithm never stops searching, the cart continues to sniff around the light source. For $t \in [15, 30]$, the light source is slowly moved in parallel along of the track and is quickly followed by the cart. Surprisingly, the light intensity and the amplitude of the oscillations are kept practically constant as shown in Figs. 11 and 14, respectively.

Fig. 13 depicts the position of the cart throughout the experiments. From $t = 0$ to 4 seconds, the cart remains nearly stationary. Once the photosensor detects the light source, the cart promptly moves towards it, initiating oscillations with diminishing amplitudes around the light source until reaching a final residual set point denoted as $O(r)$. As the ESC algorithm continuously searches, the cart persists in probing around the light source. Between $t = 15$ and 30 seconds, the light source gradually shifts parallel along the track, swiftly trailed by the cart. Remarkably, both the light intensity and oscillation amplitude remain practically constant, as evidenced in Figs. 11 and 14, respectively.

The straightforward servomechanism facilitated a concise delineation of the controller design and enabled the assessment of closed-loop performance in real experimental scenarios involving disturbances (such as dry friction, varying lighting conditions), measurement noise, unmodeled dynamics, and significant uncertainties.

The videos of the experiments can be found in the following link: <https://bitily.me/eTUXE>.

6 | CONCLUSIONS

A novel extremum seeking control scheme, incorporating monitoring functions, norm state estimation and time-scaling has been derived for a class of uncertain nonlinear plants. This approach ensures the global convergence of the system output to a small neighborhood of the extremum point using only output feedback. Simulation results have been conducted to illustrate the controller performance, even in scenarios involving local extrema. To our knowledge, real-time solutions with global convergence properties, exclusively based on output feedback, did not exist. This paper addresses this gap and introduces a solution. Furthermore, we establish that our extremum seeking controller, based on monitoring functions, touches on engineering applications, including the localization and tracking of a light source. The theoretical results are evaluated through successful experimental tests in a one-dimensional source seeking problem. This problem involves the control of a linear servomechanism cart without the use of position/velocity measurements. The generalization of the proposed method to higher-order real-time optimization schemes involving gradient and Hessian estimates [52, 53, 54] of the map rather than using only its output measurement seems to be an interesting topic for future investigation.

Aknowlegments

This study was financed in part by the Coordenação de Aperfeiçoamento de Pessoal de Nível Superior - Brasil (CAPES) Finance Code 001; Conselho Nacional de Desenvolvimento Científico e Tecnológico, CNPq; Fundação de Amparo à Pesquisa do Estado do Rio de Janeiro, FAPERJ.

References

- [1] Tan Y, Moase WH, Manzie C, Nesić D, Mareels IMY. Extremum seeking from 1922 to 2010. 29th Chinese Control Conference (CCC) 2010;p. 14–26.
- [2] Adetola V, Dehaan D, Guay M. Adaptive extremum-seeking receding horizon control of nonlinear systems. American Control Conference, 2004 Proceedings of the 2004 2004;4:2937–2942.
- [3] Capello E, Wada T, Punta E, Fujisaki Y. Trade-off between power extraction maximisation and fatigue reduction in wind farms via second-order sliding mode control and min–max optimisation. IET Control Theory and Applications 2020;17(14):2535–2547.
- [4] Oliveira TR, Krstić M. Extremum Seeking through Delays and PDEs. SIAM; 2022.
- [5] Paz P, Oliveira TR, Pino AV, Fontana AP. Model-Free Neuromuscular Electrical Stimulation by Stochastic Extremum Seeking. IEEE Transactions on Control Systems Technology 2020;28(1):238–253.
- [6] Oliveira TR, Rodrigues VHP, Krstić M, Basar T. Nash Equilibrium Seeking in Quadratic Noncooperative Games Under Two Delayed Information-Sharing Schemes. J Optim Theory Appl 2021;191:700–735.
- [7] Pessoa RWS, Mendes F, Oliveira TR, Oliveira-Esquerre K, Krstic M. Numerical optimization based on generalized extremum seeking for fast methane production by a modified ADM1. Journal of Process Control 2019;84:56–69. <https://www.sciencedirect.com/science/article/pii/S0959152419306481>.
- [8] Oliveira TR, Feiling J, Koga S, Krstić M. Extremum seeking for unknown scalar maps in cascade with a class of parabolic partial differential equations. International Journal of Adaptive Control and Signal Processing 2020;35(7):1162–1187.

- [9] Oliveira TR, Krstic M. Extremum Seeking Feedback With Wave Partial Differential Equation Compensation. *Journal of Dynamic Systems, Measurement, and Control* 2021 10;143(4):041002. <https://doi.org/10.1115/1.4048586>.
- [10] Yu H, Koga S, Oliveira TR, Krstic M. Extremum Seeking for Traffic Congestion Control With a Downstream Bottleneck. *Journal of Dynamic Systems, Measurement, and Control* 2021 10;143(3):031007. <https://doi.org/10.1115/1.4048781>.
- [11] Olalla C, Arteaga MI, Leyva R, Aroudi AE. Analysis and Comparison of Extremum Seeking Control Techniques. In: 2007 IEEE International Symposium on Industrial Electronics, Vigo, Spain, 2007; 2007. p. 72–76.
- [12] Ariyur KB, Krstić M. *Real-Time Optimization by Extremum-Seeking Control*. John Wiley & Sons; 2003.
- [13] Krstić M, Wang HH. Stability of extremum seeking feedback for general nonlinear dynamic systems. *Automatica* 2000;36(4):595–601.
- [14] Garone CLE, Kinnaert M. Sub-optimal extremum seeking control for static maps. *IET Control Theory and Applications* 2018;12(6):745–752.
- [15] Tan Y, Nesić D, Mareels IMY. On non-local stability properties of extremum seeking control. *Automatica* 2006;42(6):889–903.
- [16] Tan Y, Nesić D, Mareels IMY, Astolfi A. On global extremum seeking in the presence of local extrema. *Automatica* 2009;45(1):245–251.
- [17] Oliveira TR, Peixoto AJ, Hsu L. Global real-time optimization by output-feedback extremum-seeking control with sliding modes. *Journal of Franklin Institute* 2012;349(4):1397–1415.
- [18] Korovin SK, Utkin VI. Using sliding modes in static optimization and nonlinear programming. *Automatica* 1974;10(5):525–532.
- [19] Pan Y, Özgüner U, Acarman T. Stability and performance improvement of extremum seeking control with sliding mode. *International Journal of Control* 2003;76(9):968–985.
- [20] Oliveira TR, Peixoto AJ, Nunes EVL, Hsu L. Control of uncertain nonlinear systems with arbitrary relative degree and unknown control direction using sliding modes. *Int J Adapt Control Signal Process* 2007;21:692–707.
- [21] Yan L, Hsu L, Costa RR, Lizarralde F. A Variable structure model reference robust control without a prior knowledge of high frequency gain sign. *Automatica* 2008;44(4):1036–1044.
- [22] Oliveira TR, Peixoto AJ, Hsu L. Sliding Mode Control of Uncertain Multivariable Nonlinear Systems With Unknown Control Direction via Switching and Monitoring Function. *IEEE Trans Automat Contr* 2010;55(4):1028–1034.
- [23] Oliveira TR, Hsu L, Peixoto AJ. Output-feedback global tracking for unknown control direction plants with application to extremum-seeking control. *Automatica* 2011;47(9):2029–2038.
- [24] Morse AS. A three-dimensional universal controller for the adaptive stabilization of any strictly proper minimum-phase system with relative degree not exceeding two. *IEEE Trans Automat Contr* 1985;30(12):1188–1191.
- [25] Morse AS. A $4(n + 1)$ -dimensional model reference adaptive stabilizer for any relative degree one or two, minimum phase system of dimension n or less. *Automatica* 1987;23(1):123–125.
- [26] Miyasato Y. A model reference adaptive controller for systems with uncertain relative degrees r , $r + 1$ or $r + 2$ and unknown signs of high-frequency. *Automatica* 2000;36(6):889–896.
- [27] Bartolini G, Pisano A, Usai E. On an output-feedback stabilization problem with uncertainty in the relative degree. *International Journal of Robust and Nonlinear Control* 2008;36(6):741–755.

- [28] Levant A. Higher-order sliding modes, differentiation and output-feedback control. *International Journal of Control* 2008;76(9-10):924–941.
- [29] M T Angulo AL L Fridman. Output-feedback finite-time stabilization of disturbed LTI systems. *Automatica* 2012;48(4):606–611.
- [30] Fridman L, Shtessel Y, Edwards C, Yan XG. Higher-order sliding-mode observer for state estimation and input reconstruction in nonlinear systems. *International Journal of Robust and Nonlinear Control* 2008;18(4-5):399–412.
- [31] Bartolini G, Ferrara A, Usai E. Chattering avoidance by second order sliding mode control. *IEEE Trans Automat Contr* 1998;43(4):241–246.
- [32] Ghods N. Extremum Seeking for Mobile Robots. PhD thesis, Dept. of Mechanical and Aerospace Engineering; 2011.
- [33] Zhang C, Arnold D, Ghods N, Siranosian A, Krstić M. Source seeking with nonholonomic unicycle without position measurement and with tuning of forward velocity. In: *Proceedings of the 45th IEEE Conference on Decision and Control San Diego, CA, USA: The organization; 2006. p. 3040–3045.*
- [34] Cochran NJ, Ghods AS, Krstić M. 3D source seeking for underactuated vehicles without position measurement. *IEEE Trans on Robotics* 2009;25(1):117 – 129.
- [35] Zhang L, Deng J, Zhou K, Yu T, Song J, He S. Time-sensitive coverage control for non-holonomic and heterogeneous robots: An extremum seeking framework and application. *IET Control Theory & Applications* 2023;17(14):1909–1918.
- [36] Ghods N, Krstić M. Source seeking with very slow or drifting sensors. *J Dyn Sys, Meas, Control* 2011;133(4):044504 (8 pages).
- [37] Fu L, Özgüner U. Extremum-seeking control in constrained source tracing with nonholonomic vehicles. *IEEE Trans on Ind Electronics* 2011;56(9):3602 – 3608.
- [38] Cochran J, Kanso E, Kelly SD, Xiong H, Krstić M. Source seeking for two nonholonomic models of fish locomotion. *IEEE Trans on Robotics* 2009;25(5):1166 – 1176.
- [39] Aminde NO, Oliveira TR, Hsu L. Output-Feedback Extremum Seeking Control via Monitoring Functions. In: *52nd IEEE Conference on Decision and Control (CDC); 2013. p. 1031–1036.*
- [40] Oliveira TR, Aminde NO, Hsu L. Monitoring Function based Extremum Seeking Control for Uncertain Relative Degrees with Light Source Seeking Experiments. In: *53rd IEEE Conference on Decision and Control (CDC); 2014. p. 3456–3462.*
- [41] Khalil HK. *Nonlinear Systems*. 3 ed. Prentice Hall; 2002.
- [42] Filippov AF. Differential equations with discontinuous right-hand side. *American Math Soc Translations* 1964;42(2):199–231.
- [43] Krichman M, Sontag ED, Wang Y. Input-output-to-state stability. *SIAM J Contr Optim* 2001;39(6):1874–1928.
- [44] Zhang C, Siranosian A, Krstić M. Extremum seeking for moderately unstable systems and for autonomous vehicle target tracking without position measurements. In: *American Control Conference; 2006. p. 1832–1839.*
- [45] Utkin V, Guldner J, Shi J. *Sliding mode control in electromechanical systems*. Taylor & Francis Ltd; 1999.
- [46] Kokotović P, Khalil HK, O'Reilly J. *Singular perturbation methods in control: analysis and design*. SIAM; 1986.
- [47] Costa RR, Hsu L. Unmodeled dynamics in adaptive control systems revisited. *Systems & Control Letters* 1991;16(5):341–348.
- [48] Costa RR, Hsu L. Robustness of VS-MRAC with respect to unmodeled dynamics and external disturbances. *International Journal of Adaptive Control and Signal Processing* 1992;6(1):19–33.

- [49] Moya P, Ortega R, Netto MS, Praly L, Picó J. Application of nonlinear time-scaling for robust controller design of reaction systems. *International Journal of Robust and Nonlinear Control* 2002;12(1):57–69.
- [50] Levant A. Finite-time stability and high relative degrees in sliding-mode control. In: *Sliding Modes after the First Decade of the 21st Century, Lecture Notes in Control and Information Sciences*; 2012. p. 59–92.
- [51] Hirschorn RM. Chattering avoidance by second order sliding mode control. *IEEE Trans Automat Contr* 2001;46(2):276–285.
- [52] Rušiti D, Evangelisti G, Oliveira TR, Gerdtts M, Krstić M. Stochastic Extremum Seeking for Dynamic Maps With Delays. *IEEE Control Systems Letters* 2019;3(1):61–66.
- [53] Oliveira TR, Krstić M. Newton-based Extremum Seeking under Actuator and Sensor Delays. *IFAC-PapersOnLine* 2015;48(12):304–309. <https://www.sciencedirect.com/science/article/pii/S2405896315014986>, 12th IFAC Workshop on Time Delay Systems TDS 2015.
- [54] Ghaffari A, Krstić M, Nešić D. Multivariable Newton-based extremum seeking. *Automatica* 2012;48(8):1759–1767. <https://www.sciencedirect.com/science/article/pii/S0005109812002324>.